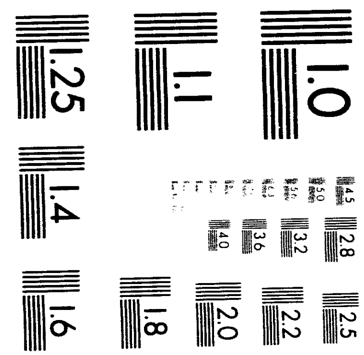
1.0
1.1
1.25
1.4
1.6
1.8
2.0
2.2
2.5
2.8
3.2
3.6
4.0
4.5
5.0

1 of 1

Conf-931142--2

LA-UR- 93-3614

Title: THE FRACTURE BEHAVIOR OF A CVD CRYSTALLINE SILICON NITRIDE/ AMORPHOUS SILICON NITRIDE COMPOSITE

Author(s): I. E. Reimanis, J. J. Petrovic, H. Suematsu, and T. E. Mitchell

Submitted to: American Ceramic Society, Honolulu, HI
November 7-10, 1993

MASTER

Los Alamos
NATIONAL LABORATORY

THE FRACTURE BEHAVIOR OF A CVD CRYSTALLINE Si_3N_4/AMORPHOUS Si_3N_4 COMPOSITE

I. E. Reimanis, J. J. Petrovic, H. Suematsu and T. E. Mitchell
Los Alamos National Laboratory, Los Alamos, NM 87545

ABSTRACT

The mechanical properties of a chemically vapor deposited α-Si_3N_4/amorphous Si_3N_4 composite were examined at 25°C and up to 1400°C using a microhardness tester. The composite consists of an amorphous matrix containing elongated α-Si_3N_4 particles (5 - 50 μm in diameter) which in some cases are radially microcracked. The conditions for spontaneous microcracking due to thermal residual stress are derived for a cylinder embedded in a matrix. Heat treatment of the composite at 1200°C results in a microstructure where the matrix consists of nanometer-sized particles separated by thin (50 Å) layer of carbon. The indentation fracture toughness of the heat treated material improves remarkably due to extended microcracking through the carbon layer.

INTRODUCTION

The ambient and high temperature deformation of monolithic and composite Si_3N_4 has been studied extensively by the structural ceramics community. Grain boundaries and bimaterial interfaces are critical in controlling the high temperature mechanical properties of Si_3N_4-based materials though mechanisms such as grain boundary sliding, crack deflection, microcrack toughening and particle pullout [1, 2]. Amorphous Si_3N_4 is used by the electronics industry in its amorphous state as a passivation layer [3, 4]. However, there has been relatively little reported on the mechanical properties of amorphous Si_3N_4 [4, 5].

In the following, we report on the mechanical properties of a Si_3N_4 composite consisting of large particles of α-Si_3N_4 embedded in an amorphous matrix. The tailorability of the as-deposited microstructure by heat treatment is discussed with respect to the mechanical properties evaluated using indentation techniques.

EXPERIMENTAL

Amorphous Si_3N_4 was chemical vapor deposited on a graphite mandrel approximately 10 mm in diameter, using a mixture of $HSiCl_3$, NH_3 and H_2 at 1200°C. Details of the CVD process are reported elsewhere [6]. The initial one or two millimeters of material are typically amorphous. Continued deposition results in the growth of cylindrical α-Si_3N_4 particles which are surrounded by amorphous Si_3N_4. Specimens were heat-treated at 1400°C for 1 hour in a N_2 environment.

The indentation fracture toughness and hardness were measured by placing Vickers indentations at various loads on sections which were ground and polished using diamond media down to 1 μm diamond. Sections were only taken from areas containing the α-Si_3N_4 particles. The indentations were carried on a Nikon QM-2 microhardness tester with a temperature range from 25°C to 1200°C. The fracture toughness values were calculated from indentations, assuming a penny-shaped crack and using the analysis of Anstis et al. [8].

RESULTS AND DISCUSSION

Spontaneous Microcracking in Cylindrical Particles

The as-deposited microstructure contains α-Si_3N_4 particles as confirmed by x-ray diffraction [7]. These particles are elongated in the direction of the deposition, with an aspect ratio varying from 3 to 7. Particles with a diameter larger than about 20 μm contain radial microcracks as shown in the optical micrograph in figure 1a, and schematically in figure 1b. It is likely that the particles are in residual tension due to the thermal expansion mismatch between the particle and the matrix during cooling from the CVD temperature (1200°C). Assuming the particles are completely surrounded by the matrix during cooling, and using a value of $1.6 \times 10^{-6}{}^\circ C^{-1}$ for the thermal expansion coefficient (TCE) of amorphous α-Si_3N_4 [9], and $2.9 \times 10^{-6}{}^\circ C^{-1}$ for the TCE of the cylindrical particle [10], the magnitude of the residual stress may be calculated. Taking 300 GPa for the elastic modulus of Si_3N_4, the thermal residual stress is $\sigma_r = E\,\Delta\alpha\,\Delta T = 470$ MPa.

The degree of spontaneous microcracking may determine the strength of the composite. Thus, the conditions under which spontaneous microcracking occurs are derived. The following adapts an analysis by Green [11] for spherical particles to the present case of cylindrical particles.

For a thick-walled cylinder in tension (figure 1b), the radial and tangential stresses (σ_{rr} and $\sigma_{\Theta\Theta}$) are given by [12]

$$\sigma_{rr} = \sigma_r\,(r^2/R^2) \qquad (1)$$

$$\sigma_{\Theta\Theta} = -\,\sigma_{rr} \qquad (2)$$

where R is the radius of the cylinder and r is the radial position (figure 1b). Assuming an axisymmetric stress field the stress intensity factor is given by [13]

$$K_I = 2/(\pi\,a)^{1/2} \int_0^a \sigma(r)\,r/(a^2 - r^2)^{1/2}\,dr \qquad (3)$$

When $a < R$, $\sigma(r) = \sigma_r$, then (3) becomes

$$K_I = 2\,\sigma_r\,(a)^{1/2}/(\pi)^{1/2} \qquad (4)$$

Equation (4) is identical for the case when the inclusion is a sphere. When $a > R$, $\sigma(r) = \sigma_r$ for $r < R$ and $-\sigma_{\Theta\Theta}$ for $r > R$, and equation (3) becomes

$$K_I = 2\,\sigma_r\,(a)^{1/2}/(\pi)^{1/2}\,[1 - (a^2 - r^2)^{1/2}/a + r^2/a^2\,(\log\,(a - (a^2 - r^2)^{1/2})/r] \quad (5)$$

The results, namely, equations (4) and (5) are shown in figure 2. Figure 2 allows one to calculate the size of crystals for which spontaneous microcracking will occur. The spontaneous microcracking criterion depends on the size of the largest internal flaw in the particle. For example, flaw sizes less than or equal to 10 μm would not extend in a 10 μm size particle, but a 10 μm size flaw in a 50 μm particle would extend to a length just over 50 μm. Provided that some cracking occurs with an applied stress, the toughness may be enhanced by stress-induced microcracking. Thus, an optimum ~~structural~~ microstructure would contain particle sizes less than the critical size for spontaneous microcracking, but greater than the critical size for stress-induced microcracking.

Mechanical Properties and Microstructure

The indentation fracture toughness does not vary significantly with temperature in the as-deposited material, as may be seen in figure 3 where the Vickers hardness is also shown. Crack patterns from the indentation are generally straight and planar and are not perturbed by the α-Si_3N_4 particles, except when they are in close proximity to the particle (figure 4). Particle/matrix debonding was only observed in cases where the interface was located in the path of the crack (e.g., figure 4). Transmission electron microscopy of the as-deposited material revealed that the matrix is entirely amorphous consisting of Si and N. No carbon was detected using EELS.

The heat treatment produces a microstructure consisting of nanometer size particles of α-Si_3N_4 and in some cases β-Si_3N_4. The transmission electron micrographs in figure 5 illustrates these significant microstructural changes. Using EELS carbon was detected in pockets and at grain boundaries. Some TEM specimens contained cracks which had clearly propagated through the carbon (figure 5). Details of these microstructural and mechanical properties observations are discussed elsewhere [7]. As observed in the TEM, all of the matrix material is either fine-grained Si_3N_4 or carbon. The carbon offers a path of low fracture resistance, resulting in the tortuous indentation crack paths observed in the indentation studies. The indentation fracture toughness was measured to be 4.4 ± 1.0 MPa(m)$^{1/2}$, compared with 1.9 ± 0.4 MPa(m)$^{1/2}$ for the as-deposited specimen. The only possible source of carbon is the graphite mandrel which was used in the deposition process. While no carbon was detected in the as-deposited material, it is likely that some diffusion of carbon occured during the heat treatment, thereby contaminating the crystallized Si_3N_4.

CONCLUSIONS

The conditions for spontaneous microcracking in a cylindrical particle have been derived. Depending on the maximum flaw sizes, the strength of the α-Si_3N_4-amorphous Si_3N_4 composite is optimized by reducing the cylindrical particle size below the critical size for spontaneous microcracking (figure 2). Heat treatment of the material results in a fine grained (nanometer size) microstructure which exhibits a higher indentation fracture toughness than the as-deposited material. It is likely that carbon plays a role in affecting the fracture behavior by offering paths of low fracture resistance (figure 5).

ACKNOWLEDGEMENTS
The authors would like to acknowledge the Department of Energy's Office of Basic Energy Sciences, Division of Materials Science, for supporting this work

REFERENCES

[1] M. J. Hoffman and G. Petzow, Mat. Res. Soc. Symp. Proc. vol 287, page 3 (1993).

[2] P. F. Becher J. Amer. Ceram. Soc. Vol. 74, pp. 255 - 269 (1991).

[3] P. S. Peercy and H. J. Stein, Proc. Symp. on Silicon Nitride Thin Insulating Films, eds. V. J. Kapoor and H. J. Stein, The Electrochemical Society, Pennington, (1983).

[4] V. I. Belyi, L L. Vasilyeva, A. S. Ginovker, V. A. Gritsenko, S. M. Repensky, S. P. Sinitsa, T. P. Smirnova and F. L. Edelman, Materials Science Monographs 34, Silicon Nitride in Electronic materials, Elsevier, NY (1988).

[5] K. Niihara and T. Hirai, J. Mater. Sci. 12, p. 1243 (1977).

[6] J. W. Lennartz and M. B. Dowell "CVD of Silicon Nitride Plate from $HSiCl_3$-NH_3-H_2 Mixtures, MRS 1988.

[7] I. E. Reimanis, J. J. Petrovic, H. Suematsu and T. E. Mitchell, to be published.

[8] G. R. Anstis, P. Chantikul, B. R. Lawn and D. B. Marshall J. Amer. Ceram. Soc. Vol. 64, No. 9, pp. 533 - 538 (1981).

[9] T. F. Retajczyk and A. K. Sinha Thin Solid Films, 70 pp. 241 - 247 (1980).

[10] C. M. B. Henderson and D. Taylor, *Trans. J. Br. Ceram. Soc.* 74(2), p. 49, (1975).

[11] D. J. Green in Fracture Mechanics of Ceramics, vol. 5, eds. R. C. Bradt, A. G. Evans, D. P. Hasselman and F. F. Lange, pp. 457-478, Plenum Press, NY (1983).

[12] J. W. Dally and W. F. Riley Experimental Stress Analysis, 2nd Edition page 73, McGraw-Hill Inc., NY (1978).

[13] G. C. Sih, Handbook of Stress Intensity Factors, copyright G. C. Sih, (1973).

FIGURES

Figure 1 **a**. Optical micrograph of spontaneously cracked α-Si_3N_4 particle. **b.** Schematic of cracked cylinder under hydrostatic pressure

Figure 2 Stress intensity factor as a function of normalized flaw size. The critical stress intensity factor for the particle and for the matrix are shown as dotted lines.

Figure 3 Fracture toughness and Vickers hardness as a function of temperature for the as-deposited material.

Figure 4 Optical micrograph of α-Si_3N_4 particle in the vicinity of a Vickers indentation in the as-deposited material. Note what appears to be some debonding between the particle and the matrix.

Figure 5 Transmission electron micrograph of the heat treated material, showing the fine grained microstructure with regions of carbon.

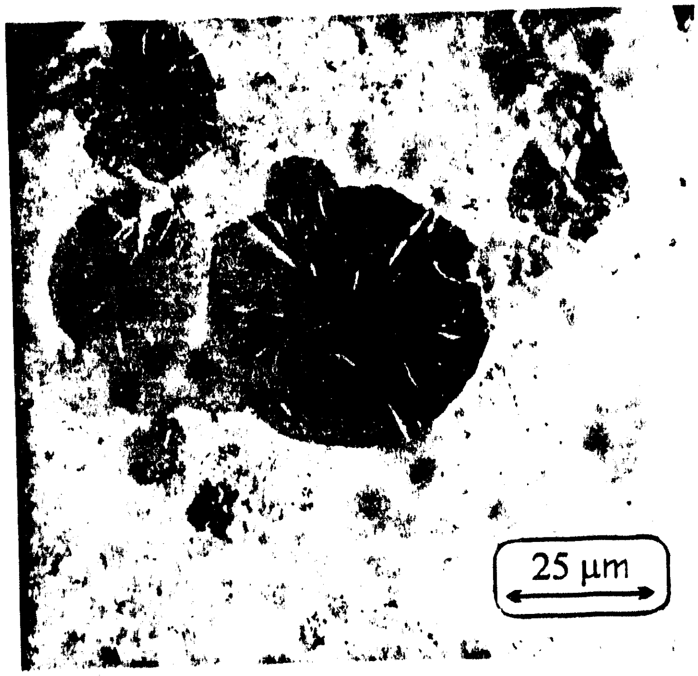

Figure 1(a)

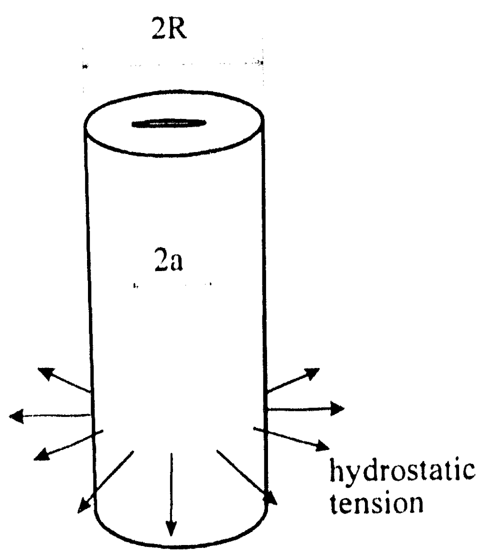

Figure 1(b)

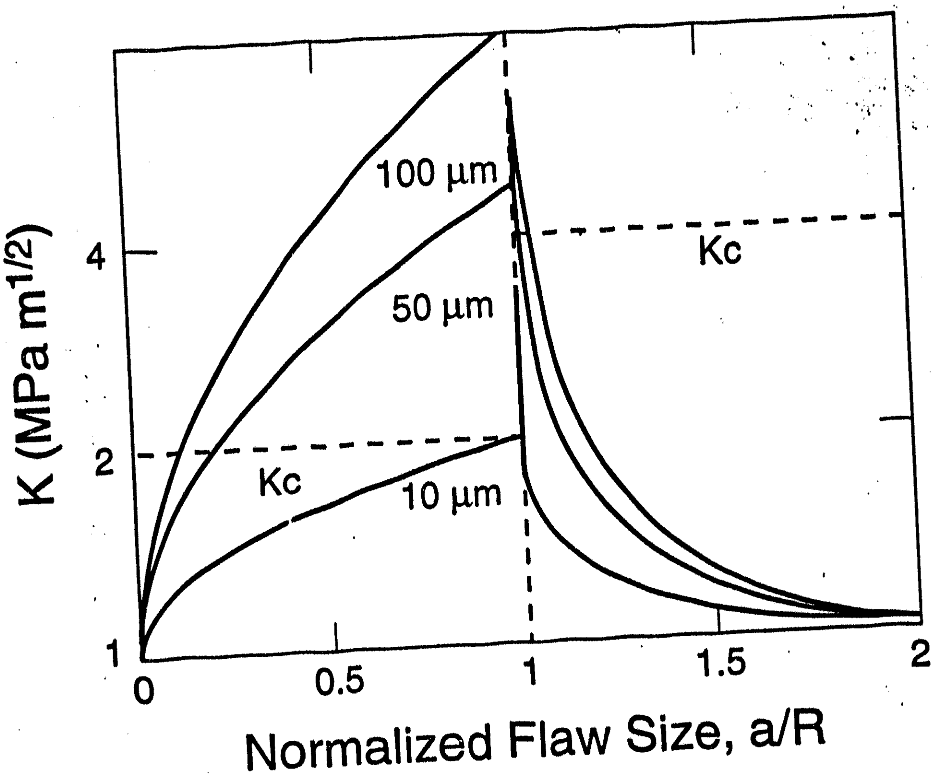

Figure 2

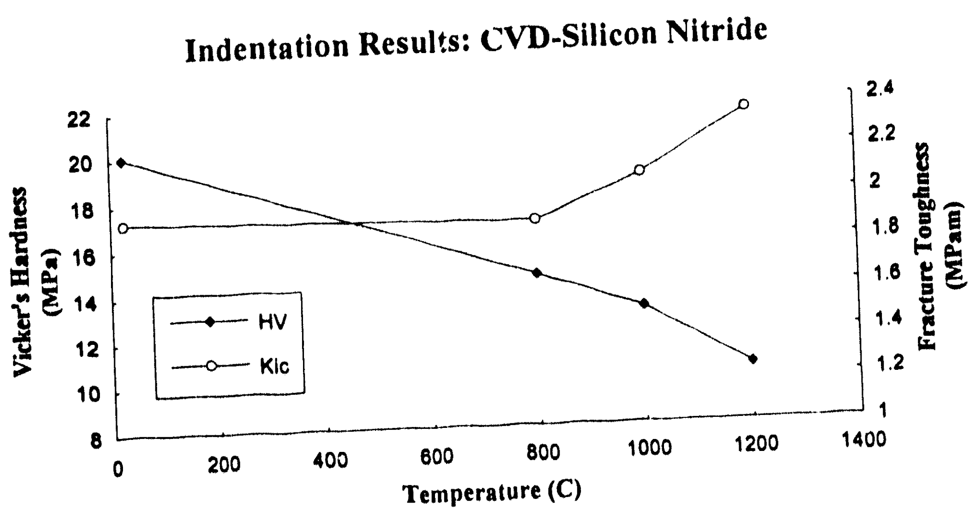

↑

This is being "smoothed over" at IS-1
9/29/93

Figure 3

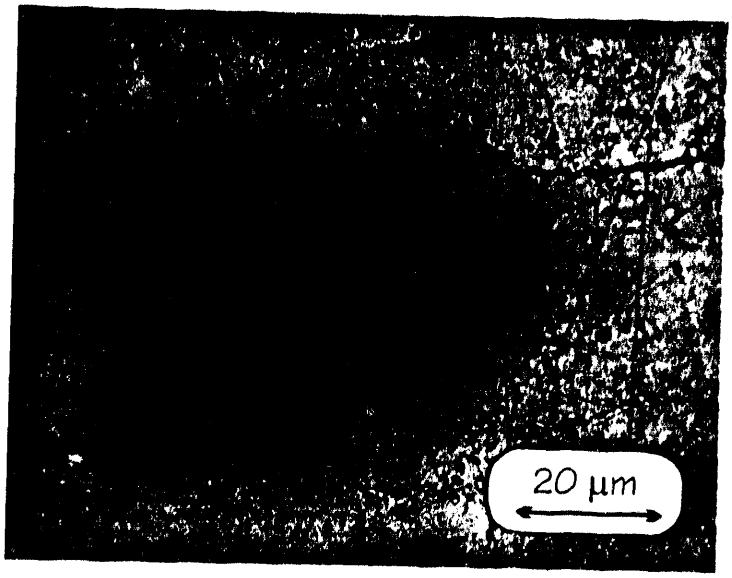

Figure 4

Figure 5

DATE FILMED

1 / 21 / 94

END